Optimizations of Defect Filter Layers for 1.3-μm InAs/GaAs Quantum-Dot Lasers Monolithically Grown on Si Substrates

Mingchu Tang, *Student Member, IEEE*, Siming Chen, *Member, IEEE*, Jiang Wu, Qi Jiang, Ken Kennedy, Pamela Jurczak, Mengya Liao, *Student Member, IEEE*, Richard Beanland, Alwyn Seeds, *Fellow, IEEE*, and Huiyun Liu

***Abstract*—III–V semiconductors monolithically grown on Si substrates are expected to be an ideal solution to integrate highly efficient light-emitting devices on a Si platform. However, the lattice mismatch between III–V and Si generates a high density of threading dislocations (TDs) at the interface between III–V and Si. Some of these TD will propagate into the III–V active region and lead to device degradation. By introducing defect filter layers (DFLs), the density of TDs propagating into the III–V layers can be significantly reduced. In this paper, we present an investigation on the development of InGaAs/GaAs strained-layer superlattices as DFLs for 1.3-μm InAs/GaAs quantum-dot lasers monolithically grown on a Si substrate. We compare two broad-area InAs/GaAs quantum-dot lasers with non-optimized and optimized InGaAs/GaAs DFLs. The laser device with optimal DFLs has a lower room-temperature threshold current density of 99 A/cm^2 and higher maximum operation temperature of 88 °C, compared with 174 A/cm^2 and 68 °C for the reference laser.**

***Index Terms*—Molecular beam epitaxy, quantum dots, semiconductor lasers, silicon photonics.**

I. Introduction

In order to achieve fast chip-to-chip and system-to-system optical communication with Si photonic integrated circuits, Si–based efficient and reliable light emitting sources are required. A Si–based light-emitting source has long been considered the "holy grail" of Si photonics because of the challenges involved. Bulk Si and Ge have an indirect bandgap, and thus are not efficient light-emitting materials [1], [2]. Until now, novel approaches including hybrid/monolithic integration of III–V/Si, stimulated Raman scattering and Ge/Si laser, have been developed for silicon-based lasers. However, Si Raman lasers are restricted by the need for off-chip optical pumping [3], [4], while Ge/Si lasers suffer from extremely high threshold current density (>300 kA/cm^2) and high optical loss [5].

Recently, the heterogeneous integration of III–V semiconductors on Si platforms has demonstrated lasers with milliwatt power output and high operating temperature (>100 °C) by using wafer-bonding techniques [6]. However, the issues of yield and reliability for this approach still remain. III–V materials monolithically grown on Si substrates have been proposed as an ideal solution for photonic integration on Si, i.e., by growing GaAs or InP buffer layers directly on Si substrates [7], [8]. The major issue for this method is the formation of threading dislocations (TDs) due to the lattice and thermal expansion coefficient mismatch between the III–V materials and Si [9] and antiphase domains (APDs) due to the polar to non-polar epitaxial growth [10]. APDs can be eliminated by growing III–V materials on off-cut Si substrates and using a two-step growth method [11]. For the epitaxial growth of III–V materials on Si substrates, optimization of the buffer layers, including the GaAs buffer layer and defect filter layers (DFLs), plays a crucial role in reducing the threading dislocation density from 10^{10} cm^{-2} at the GaAs/Si interface to 10^6 cm^{-2} at the active region [12], [13]. Yang *et al.* demonstrated the pulsed operation of a 1.1 μm InAs/GaAs quantum dot (QD) laser on a Si substrate by using QD DFLs [14] and Nakamura *et al.* have used AlGaN/GaN strained-layer superlattices (SLSs) as DFLs to achieve a multi-quantum-well laser on GaN [15].

QDs possess unique properties that can lead to lasers with ultra-low threshold currents, temperature insensitivity and reduced sensitivity to TDs [16]–[22]. Therefore, a combination of high efficacy DFLs and III-V QDs has been considered to be the most attractive approach for achieving III–V/Si lasers. Indeed, based on this technique, Wang *et al*. reported the first 1.3-μm InAs/GaAs QD lasers monolithically grown on Si substrates [23], while Chen *et al.* and Jiang *et al*. demonstrated the first InAs/GaAs QD SLDs monolithically grown on Si and Ge substrates [24], [25]. Likewise, continuous-wave operation of InAs/GaAs QD lasers monolithically grown on Ge/Si substrates have been reported recently [26]–[29].

To obtain practical lasers on Si, further reduction in dislocation density in the III-V buffer layer is required, and hence more efficient DFLs are needed. In this paper, we report the optimizations of the DFLs by adjusting growth conditions and structures of InGaAs/GaAs SLSs. The optimization involves

Manuscript received January 30, 2016; revised March 10, 2016 and March 23, 2016; accepted April 01, 2016. This work was supported by UK EPSRC under Grant EP/J012904/1. The work of H. Liu was supported by the Royal Society for funding his University Research Fellowship.

M. Tang, S. Chen, J. Wu, Q. Jiang, P. Jurczak, M. Liao, A. Seeds, and H. Liu are with the Department of Electronic and Electrical Engineering, University College London, London WC1E 7JE, U.K. (e-mail: mingchu.tang.11@ucl.ac.uk; siming.chen@ucl.ac.uk; jiang.wu@ucl.ac.uk; q.jiang@ucl.ac.uk; pamela.jurczak.10@ucl.ac.uk; mengya.liao@ucl.ac.uk; a.seeds@ucl.ac.uk; huiyun.liu@ucl.ac.uk).

K. Kennedy is with the Department of Electronic and Electrical Engineering, University of Sheffield, Sheffield S1 3JD, U.K. (e-mail: k.kennedy@sheffield.ac.uk).

R. Beanland is with the Department of Physics, University of Warwick, Coventry CV4 7AL, U.K. (e-mail: R.Beanland@warwick.ac.uk).

Color versions of one or more of the figures in this paper are available online at http://ieeexplore.ieee.org.

Digital Object Identifier 10.1109/JSTQE.2016.2551941

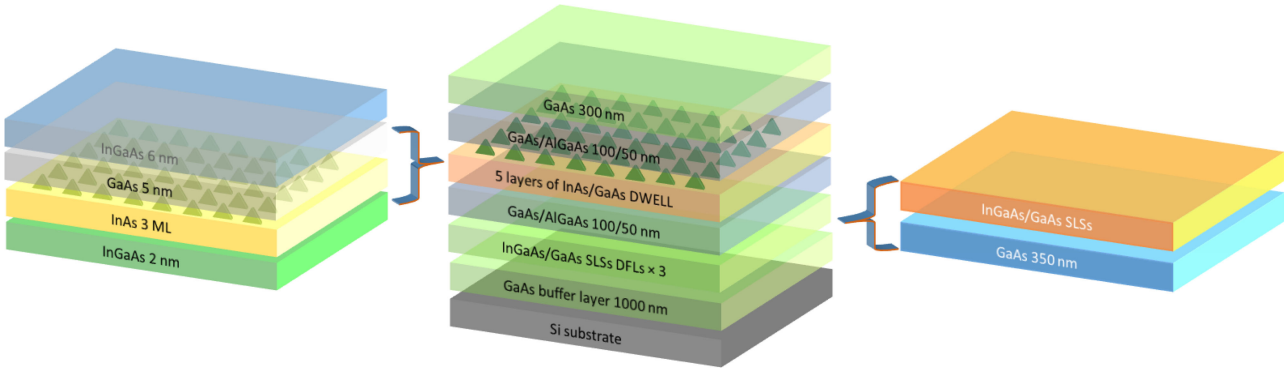

Fig. 1. Schematic diagram of InAs/GaAs QD monolithically grown on Si substrate with InGaAs/GaAs SLSs DFLs.

in-situ thermal annealing, variation of indium composition in the SLSs, and variation of GaAs thickness in the SLSs. Finally, the performance of two InAs/GaAs QD lasers monolithically grown on Si substrates under non-optimized and optimized conditions was compared. The optimization of DFLs leads to significant improvements of QD lasers, including reduction of threshold current density from 174 to 99 A/cm^2 and increase of maximum operation temperature from 66 to 88 °C.

II. Growth Structure

The QD structures were grown by solid-source molecular beam epitaxy (MBE). As shown in the schematic image in Fig. 1, five layers of InAs/GaAs QDs were monolithically grown on n-doped Si substrates (1 0 0) with 4° offcut oriented to ⟨0 1 1⟩ after introducing a 1 μm GaAs buffer layer and three sets of InGaAs/GaAs SLSs. Before the growth, oxide desorption of the Si substrate was performed at 900 °C for 30 min. The 1 μm-GaAs buffer layer was grown in two steps: low temperature growth of 30 nm GaAs with a growth rate of 0.1 monolayers/s (ML/s) at 380 °C followed by high temperature growth of 970 nm GaAs grown with 0.7 ML/s. The two-step growth helps to confine most of the TDs at the interface region. To further reduce the threading dislocation density, the three sets of InGaAs/GaAs DFLs were grown after the first 1 μm GaAs buffer. Each set of DFLs consisted of five periods of InGaAs/GaAs SLSs and separated by a 350 nm GaAs spacer layer. To improve the effectiveness of InGaAs/GaAs DFLs, we introduced two different growth methods for the DFLs. As shown in Fig. 2, in the growth method I, a GaAs spacer layer was grown during the period of heating up to 610 °C right after the deposition of InGaAs/GaAs SLSs at 420 °C. In contrast, in growth method II, GaAs spacer layer was grown after *in-situ* annealing of the SLSs at 610 °C. Additionally, the efficacy of indium composition x and GaAs thickness in the SLSs has also been studied by using $x = 0.16$, 0.18 and 0.20 for indium compositions and 8, 9 and 10 nm for GaAs thickness.

For the growth of the active region, five InAs/InGaAs dot-in-a-well (DWELL) layers were grown [30]. About 3 MLs of InAs with 0.1 ML/s growth rate were deposited on 2 nm of InGaAs and then capped by 6 nm of InGaAs and 5 nm of GaAs. The QDs were grown at 510 °C while each layer of InAs/GaAs QDs was

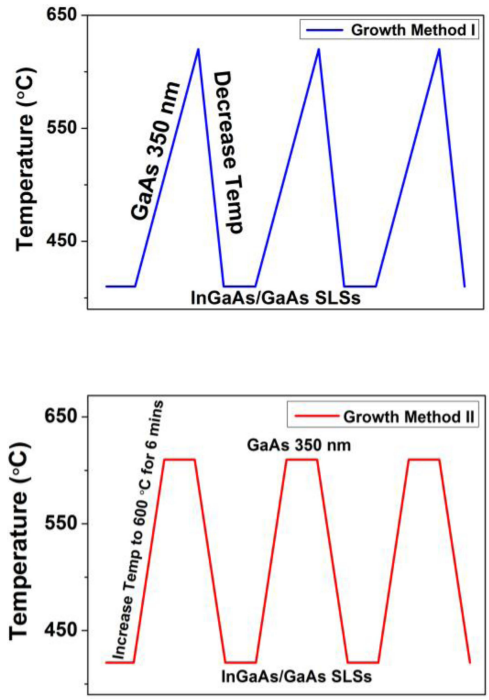

Fig. 2. Two different growth methods of DFLs. Growth method I: The GaAs spacer layer was grown during the ramp-up of temperature from 420 to 610 °C and then cooled down to 420 °C for subsequent growth of InGaAs/GaAs SLSs growth; Growth method II: The GaAs spacer layer was not grown during the ramp-up of temperature from 420 to 610 °C, and deposited only at a stable temperature of 610 °C and then cooled back to 420 °C for subsequent InGaAs/GaAs SLSs growth.

separated by 45 nm of GaAs spacer layer. The DWELLs were embedded between two 100-nm GaAs layers grown at 580 °C and 50-nm AlGaAs layers grown at 610 °C. The QD density is around 3.8 × 10^{10} cm^{-2} as presented in Fig. 3.

III. Effects of InGaAs/GaAs DFLs on the Material Qualities of III–V Materials Grown on Si Substrates

In Table I, QD densities and photoluminescence (PL) peak intensities are compared for each step of optimizations including modifying growth methods of GaAs spacer layer, indium composition and GaAs thickness in $In_xGa_{1-x}As$/GaAs DFLs.

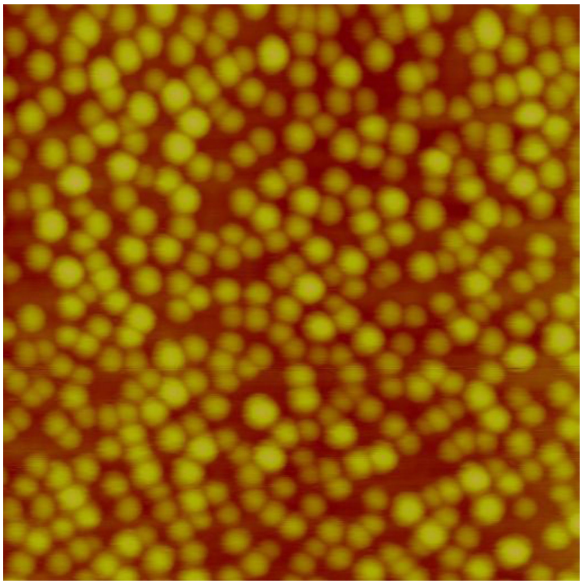

Fig. 3. AFM image of InAs/GaAs QDs monolithically grown on Si substrate, with density around 3.8×10^{10} cm^{-2}.

TABLE I
THE QD DENSITIES AND PL PEAK INTENSITIES OF SAMPLES GROWN WITH DIFFERENT GROWTH METHODS, INDIUM COMPOSITIONS AND GAAS THICKNESSES

Sample	Growth methods	$In_xGa_{1-x}As$	GaAs thickness	PL peak intensity (a.u)	FWHM (nm)
A	I	$x = 0.18$	10 nm	1.2	40.5
B	II	$x = 0.18$	10 nm	4	40.3
C	II	$x = 0.16$	10 nm	2.6	39.8
D	II	$x = 0.20$	10 nm	2.2	42
E	II	$x = 0.18$	9 nm	3.9	40.4
F	II	$x = 0.18$	8 nm	2	46.1

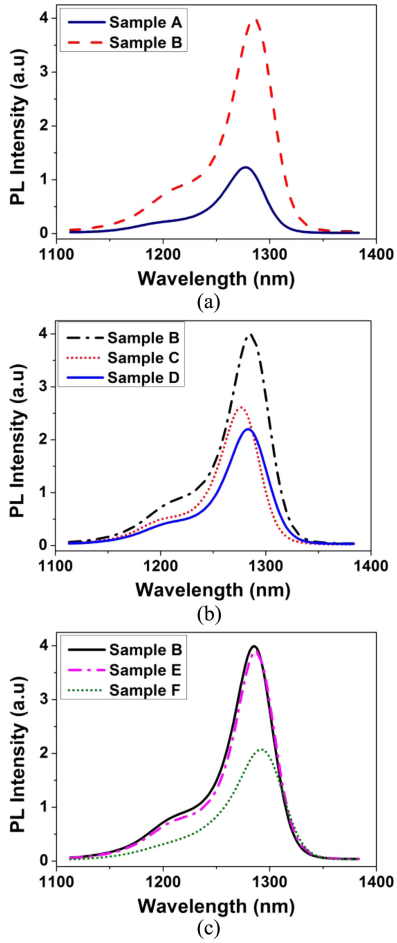

Fig. 4. PL spectra of different samples measured at room temperature: (a) sample A (growth method I) and sample B (growth method II), (b) samples B, C, and D with indium composition of 18%, 16%, and 20%, respectively, (c) samples B, E, and F with GaAs thickness of 10 nm, 9 nm and 8 nm, respectively.

Growth methods I and II have been applied to samples A and B, respectively. For the samples B, C and D, the indium composition in InGaAs/GaAs SPL has been varied from $x = 0.16$ to 0.20. Samples B, E and F have been grown using 8, 9 and 10 nm of GaAs inside each $In_xGa_{1-s_x}As$/GaAs SLS, respectively.

The PL measurements were performed using 635-nm solid-state laser excitation at room temperature. The PL spectrum in Fig. 4(a) shows that sample B has three times stronger emission of ground state than sample A. Sample B's separation between ground state and excited state is 60 meV, which is slightly larger than 56 meV of sample A. The PL measurements show an improved optical property of sample B using growth method II compared with sample A using growth method I. The reason for this improvement in PL intensity can be understood in term of the improved material quality after using *in-situ* annealing of SLSs. After the growth of InGaAs/GaAs at low temperature, the annealing of SLSs and high temperature growth of GaAs increase the dislocation motions, which helps the dislocations to meet and eliminate each other. As a result, less non-radioactive recombination is expected in the QD region due to reduced density of TDs.

As presented in Fig. 4(b), sample B exhibits PL intensity that is approximately 30% and 40% greater than samples C and D, respectively. This proves that the indium composition of 0.18 in $In_xGa_{1-x}As$/GaAs SLSs contributes the best crystal quality compared with the other indium compositions used. The remarkable improvement observed in PL intensity is due to a good balance between generation of strain-induced defects and annihilation of dislocations. A higher indium composition in InGaAs/GaAs SLSs is able to increase strain and block more TDs from propagating. On the other hand, the larger strain could introduce new TDs, and hence undermine the dislocation filtering efficiency of SLSs and degrade the structural and optical qualities of epilayers.

Cross-sectional transmission electron microscopy (TEM) measurements have been performed to examine the crystal quality further and compare the effectiveness of the DFLs of each sample. As shown in the bright-field TEM images in Fig. 5(a), a large number of dislocations appear at the interface of GaAs/Si. Most of the dislocations are trapped in the first 200 nm due to self-annihilation. However, there are still a considerable number of TDs propagating towards the active region. After

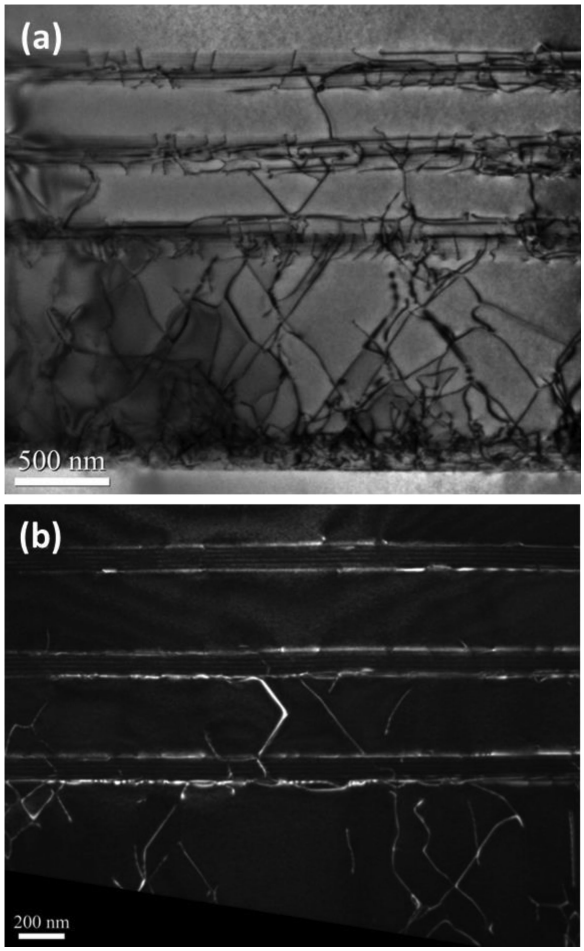

Fig. 5. (a) dark-field TEM cross-sectional TEM image of three layers of InGaAs/GaAs SLSs DFLs. (b) Bright-field TEM cross-sectional image of DFLs on GaAs buffer layer and Si substrate.

introduction of the DFLs the annihilation of TDs has been significantly enhanced. As shown in Fig. 5(a) and (b), the majority of TDs have been blocked by three sets of DFLs. As a result, the material quality and then device performance are largely dependent on the efficiency of DFLs.

To examine the efficiency of different types of DFL, we have measured dislocation density just above each layer of DFL using TEM measurements. We define the efficiency of DFL as the fraction of TDs it removes, which can be expressed as [31]

$$\text{Efficiency} = 1 - \frac{n(\text{experiment})}{n(\text{predict})} \tag{1}$$

where n(experiment) is the number of dislocations counted just above the DFL and n(predict) is the number of dislocations predicted by the equation describing "natural" decrease in ρ_{TD} [32]. The dislocation density ρ_{TD} with natural decay is related to the thickness h and can be expressed as

$$\rho_{\text{TD}} = Ah^{-0.5} \tag{2}$$

where A is a constant fitted by the counts of TDs at three positions in the GaAs buffer layer: 300, 600 and 900 nm. The efficiencies of each type of DFLs are presented in Fig. 6. For the

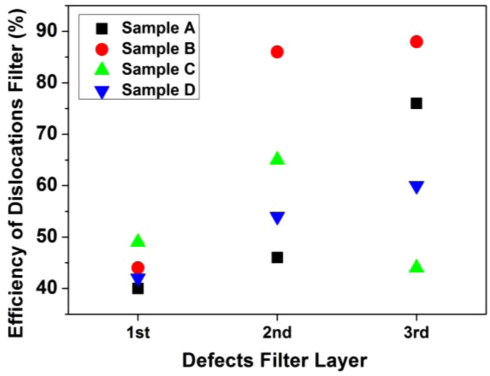

Fig. 6. Plots of sample A, B, C and D's efficiency of filtering dislocations at each set of DFLs.

first set of DFL, the efficiencies of four samples A, B, C, and D range from 40% to 50%. After the first set of DFL, samples B, C and D show a stronger increase in efficiency compared with sample A. This is due to the *in situ* thermal annealing and high temperature GaAs spacer layer growth, which successfully increase the dislocation motion and hence the opportunities for the elimination of TDs. Moreover, sample B with $In_{0.18}Ga_{0.82}As$ in the SLSs show the highest filtering efficiency for the second and third sets of DFLs. The highest efficiency observed in sample B confirms a good balance between generation of strain-induced defects and annihilation of dislocations. Compared with the other samples, the significant reduction in the efficiency of the third DFL of sample C with only 16% indium in SLSs indicates inefficient interaction between strain relaxation and TDs when only a low density of threading dislocation is presented. Therefore, the sample B with 18% indium composition in InGaAs/GaAs DFLs and growth method II has been proved to be the most effective in reducing the density of TDs.

To gain further insight into the effects of DFLs, we have also compared different thicknesses of GaAs in the InGaAs/GaAs SLSs. From Fig. 4(c) it can be observed that samples B and E have similar PL spectra but the intensity for sample F is significantly lower. This clearly shows that the 8-nm GaAs (sample F) thickness is too small and the accumulated strain degrades the material quality, leading to a drop in the PL intensity by nearly a half. The PL of samples B and E are comparable because the thicker GaAs spacers provide enough buffer for strain-induced generation of detects while maintaining suitable strain relaxation of the $In_{0.18}Ga_{0.82}As$/GaAs SLS for interacting with TDs. This is in good agreement with the TEM measurements of the samples with the same thickness but different indium compositions.

IV. Laser Fabrication and Performance

To further investigate the effect of InGaAs/GaAs SLSs DFLs, full laser structures have been grown and processed. The GaAs buffer layer and InAs/GaAs DWELL active region were grown under the same conditions as previously; samples A to F. We have grown two laser samples R1 and R2 that were based on the DFL growth conditions of samples A and B, respectively. After

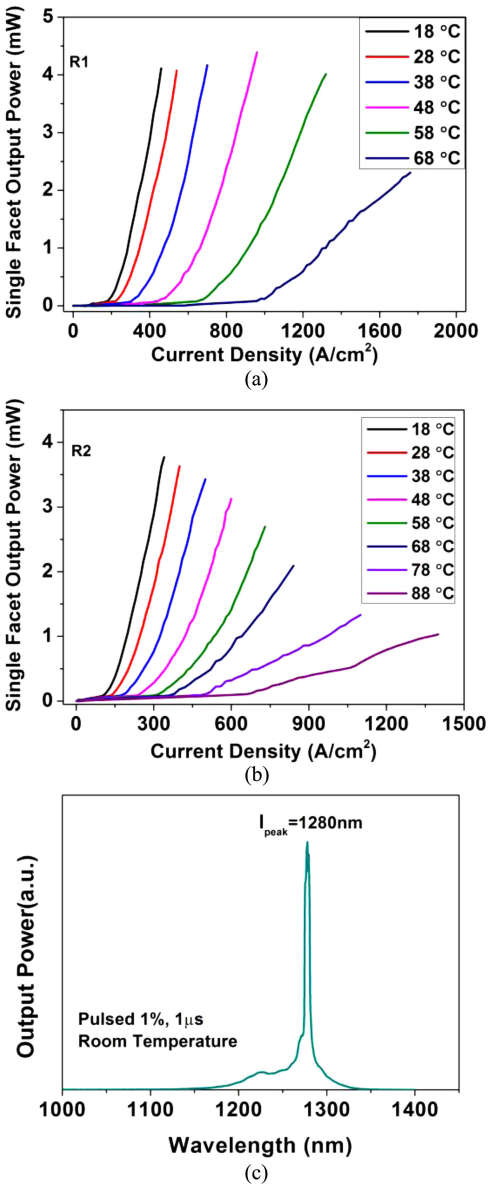

Fig. 7. Sample R1 (a) and R2 (b) Single facet output power against current density for 3-mm-long InAs/GaAs QD laser grown on Si with $In_{0.18}Ga_{0.82}As$/GaAs DFLs under pulsed mode (1% duty cycle and 1 μs pulse width) at room temperature. (c) Laser spectrum at room temperature with emission at 1280 nm.

four sets of DFLs, n and p type 1.2-μm-thick AlGaAs cladding layers were grown on the bottom and then on top of the active region.

The broad-area laser devices were fabricated. The 50 μm wide ridges were created by standard lithography and wet etching techniques. We etched down the ridges to 200 nm below the active region, so as to improve the carrier confinement. We deposited InGe/Au and Ti/Pt/Au on the GaAs n and p contact layers, respectively. Both n and p contact layers are face-up. The cavity length of the devices is 3 mm and no facet coating was applied.

Measurements of single facet output power against current density for two Si-based InAs/GaAs QD lasers are presented

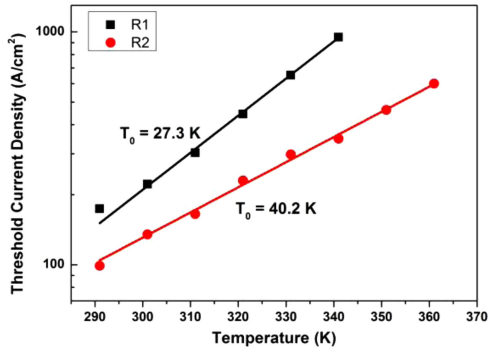

Fig. 8. Temperature dependence of the threshold current density under pulsed operation of laser sample R1 and R2.

in Fig. 7(a) and (b). During the measurements, the laser devices were mounted epi-side up with a sub-mount temperature of 18 °C without active cooling. The lasers were electrically pumped under pulsed conditions of 1% duty cycle and 1 μs pulse width. The threshold current densities of R1 and R2 are 174 and 99 A/cm^2, respectively. The lower threshold current densities from sample R2 proves that the optimized InGaAs/GaAs DFLs improve the laser performance in terms of lower threshold current density, which is due to the elimination of the majority of TDs within the GaAs buff spacer layer. The maximum operation temperature of R2 is 88 °C, which is higher than R1's maximum operation temperature of 68 °C. In addition, compared with the previous reports, sample R2 shows lower threshold current density than InAs/GaAs QD lasers on Si substrate using InAlAs/GaAs SLSs which had a threshold current of 194 A/cm^2 [13].

Fig. 7(c) shows the room-temperature lasing spectrum, which has been measured for an injection current of 105 A/cm^2. It clearly shows that the laser is emitting at 1.28 μm, which matches the PL spectrum. Fig. 8 shows the temperature dependence $J_{\rm th}$ for laser samples R1 and R2. R2 shows an improved characteristic temperature $T_0 = 40.2$ K, compared with sample R1 with $T_0 = 27.3$ K for the temperature range 18 to 68 °C. The poor performance of T_0 for R1 at the higher temperature range could be due to the increased non-radioactive recombination rate at high temperature range, due to the higher threading dislocation density compared with R2. The temperature stability of lasers can be improved by using p-type modulation doping to enhance the confinement of holes at high temperature [33].

V. Conclusion

In conclusion, we have investigated the optimization of InGaAs/GaAs SLSs DFLs by modifying (i) the GaAs spacer layer growth conditions, and (ii) the indium composition and GaAs thickness in InGaAs/GaAs SLSs. The effect of DFLs has also been studies in laser devices. The work confirms that the design and growth of DFLs play a critical role in the success of QD lasers monolithically grown on Si. Particular attention should be paid to enhancing the motion of TDs and well-controlled strain relaxation. Finally, with optimized DFLs in this work, an InAs/GaAs QD laser with a low threshold current density, high

operating temperature, and improved characteristic temperature has been demonstrated on a Si substrate. These results provide an essential step to the further improvement of the performance of InAs/GaAs QD lasers monolithically grown on a silicon platform.

REFERENCES

[1] B. Jalali and S. Fathpour, "Silicon photonics," *J. Lightw. Technol.*, vol. 24, no. 12, pp. 4600–4615, Dec. 2006.

[2] D. Liang, and E. John Bowers, "Recent progress in lasers on silicon," *Nature Photon.*, vol. 4, no. 8, pp. 511–517, 2010.

[3] H. Rong *et al.*, "An all-silicon Raman laser," *Nature*, vol. 433, pp. 292–294, 2005.

[4] H. Rong *et al.*, "A continuous-wave Raman silicon laser," *Nature*, vol. 433, pp. 725–728, 2005

[5] R. E. Camacho-Aguilera *et al.*, "An electrically pumped germanium laser," *Opt. Exp.,* vol. 20, no. 10, pp. 11316–11320, 2012.

[6] H. H. Chang *et al.*, "1310 nm silicon evanescent laser," *Opt. Exp.*, vol. 15, no. 18, pp. 11466–11471, 2007.

[7] S. M. Chen *et al.*, "1.3 μm InAs/GaAs quantum-dot laser monolithically grown on Si substrates operating over 100 °C," *Electron. Lett.*, vol. 50, no. 20, pp. 1467–1468, 2014.

[8] Z. Wang *et al.*, "Room temperature InP DFB laser array directly grown on (001) silicon," *Nature Photon.*, vol. 9, pp. 837–842, 2015.

[9] T. Ward *et al.*, "Design rules for dislocation filters," *J. Appl. Phys.*, vol. 116, no. 6, 2014, Art. no. 063508.

[10] H. Kroemer, "Polar-on-nonpolar epitaxy," *J. Crystal Growth*, vol. 81, no. 1, pp. 193–204, 1987.

[11] M. Akiyama, Y. Kawarada, and K. Kaminishi. "Growth of single domain GaAs layer on (100)-oriented Si substrate by MOCVD," *Jpn. J. Appl. Phys.*, vol. 23, no. 11, pp. L843–L845, 1984.

[12] M. Tang *et al.*, "Optimisation of the dislocation filter layers in 1.3-μm InAs/GaAs quantum-dot lasers monolithically grown on Si substrates," *IET Optoelectron.*, vol. 9, no. 2, pp. 61–64, 2015.

[13] M. Tang *et al.*, "1.3-μm InAs/GaAs quantum-dot lasers monolithically grown on Si substrates using InAlAs/GaAs dislocation filter layers," *Opt. Exp.*, vol. 22, no. 10, pp. 11528–11535, 2014.

[14] J. Yang, P. Bhattacharya, and Z. Mi, "High-performance $In_{0.5}Ga_{0.5}As$/GaAs quantum-dot lasers on silicon with multiple-layer quantum-dot dislocation filters," *IEEE Trans. Electron Devices*, vol. 54, no. 11, pp. 2849–2855, Nov. 2007.

[15] S. Nakamura *et al.*, "InGaN/GaN/AlGaN-based laser diodes with modulation-doped strained-layer superlattices grown on an epitaxially laterally overgrown GaN substrate," *Appl. Phys. Lett.*, vol. 72, no. 2, pp. 211–213, 1998.

[16] I. R. Sellers *et al.*, "1.3 μm InAs/GaAs multilayer quantum-dot laser with extremely low room-temperature threshold current density," *Electron. Lett.*, vol. 40, no. 22, pp. 1412–1413, Oct. 2004.

[17] O. B. Shchekin, and D. G. Deppe, "1.3 μm InAs quantum dot laser with T_o = 161 K from 0 to 80 °C," *Appl. Phys. Lett.*, vol. 80, no. 18 pp. 3277–3279, 2002.

[18] Y. Alan Liu *et al.*, "High performance continuous wave 1.3 μm quantum dot lasers on silicon," *Appl. Phys. Lett.*, vol. 104, no. 4, 2014, Art. no. 041104.

[19] D. Bimberg *et al.*, "InGaAs-GaAs quantum-dot lasers," *IEEE J. Sel. Topics Quantum Electron.*, vol. 3, no. 2, pp. 196–205, Apr. 1997.

[20] T. M. Crowley *et al.*, "GaAs based quantum dot lasers," *Adv. Semicond. Lasers*, vol. 86, 2012, Art. no. 371.

[21] D. Bimberg, M. Grundmann, and N. N. Ledentsov, *Quantum Dot Heterostructures*. Hoboken, NJ, USA: Wiley, 1999.

[22] G. Dennis Deppe, K. Shavritranuruk, G. Ozgur, H. Chen, and S. Freisem, "Quantum dot laser diode with low threshold and low internal loss," *Electron. Lett.*, vol. 45, no. 1, pp. 54–56, Jan. 2009.

[23] T. Wang, H. Liu, A. Lee, F. Pozzi, and A. Seeds, "1.3-μm InAs/GaAs quantum-dot lasers monolithically grown on Si substrates," *Opt. Exp.*, vol. 19, no. 12, pp. 11381–11386, 2011.

[24] S. Chen *et al.*, "InAs/GaAs quantum-dot superluminescent light-emitting diode monolithically grown on a Si substrate," *ACS Photon.*, vol. 1, no. 7, pp. 638–642, 2014.

[25] Q. Jiang *et al.*, "InAs/GaAs quantum-dot superluminescent diodes monolithically grown on a Ge substrate," *Opt. Exp.*, vol. 22, no. 19, pp. 23242–23248, 2014.

[26] A. Lee, Q. Jiang, M. Tang, A. Seeds, and H. Liu, "Continuous-wave InAs/GaAs quantum-dot laser diodes monolithically grown on Si substrate with low threshold current densities," *Opt. Exp.*, vol. 20, no. 20, pp. 22181–22187, 2012.

[27] Y. Alan Liu *et al.*, "Reliability of InAs/GaAs quantum dot lasers epitaxially grown on silicon," *IEEE J. Sel. Topics Quantum Electron.*, vol. 21, no. 6, Nov./Dec. 2015, Art. no. 1900708.

[28] H. Y. Liu *et al.*, "Optimizing the growth of 1.3 μm InAs/InGaAs dots-in-a-well structure," *J. Appl. Phys.*, vol. 93, no. 5, pp. 2931–2936, 2003.

[29] S. Chen *et al.*, "Electrically pumped continuous-wave III–V quantum dot lasers on silicon," *Nature Photon.*, to be published, doi:10.1038/nphoton.2016.21.

[30] H. Y. Liu *et al.*, "Improved performance of 1.3 mum multilayer InAs quantum-dot lasers using a high-growth-temperature GaAs spacer layer," *Appl. Phys. Lett.*, vol. 85, no. 5, 2004, Art. no. 704.

[31] I. George *et al.*, "Dislocation filters in GaAs on Si," *Semicond. Sci. Technol.*, vol. 30, no. 11, 2015, Art. no. 114004.

[32] A. E. Romanov, W. Pompe, G. Beltz, and J. S. Speck, "Modeling of threading dislocation density reduction in heteroepitaxial layers I. Geometry and crystallography," *Phys. Status Solidi (b)*, vol. 198, no. 2, pp. 599–613, 1996.

[33] HY Liu *et al.*, "p-doped 1.3 μm InAs/ GaAs quantum-dot laser with a low threshold current density and high differential efficiency," *Appl. Phys. Lett.*, vol. 89, no. 7, 2006, Art. no. 073113.

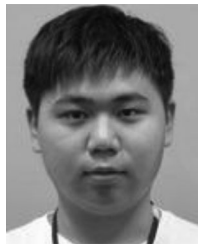

Mingchu Tang received the B.Eng. degree in electronic and electrical engineering from the University of Sussex, Brighton, U.K., in 2011 and the M.Sc. degree in nanotechnology from the University College London, London, U.K., in 2012. In October 2012, he joined the Photonics group as a Ph.D. student on Molecular Beam Epitaxy of III–V compound semiconductors and optoelectronic devices. His interest include III–V quantum dot optoelectronic devices monolithically grown on group III–V and IV platforms.

Siming Chen received the Ph.D. degree in electrical engineering from the University of Sheffield, Sheffield, U.K., in 2014. In 2013, he joined the Department of Electronic and Electrical Engineering, University College London, London, U.K., where he is currently a Research Associate. He has been working on III–V and Si based quantum dot optoelectronics devices, and silicon photonics.

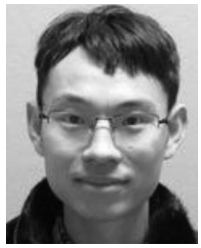

Jiang Wu received the B.S. degree from the University of Electronic Science and Technology of China, Chengdu, China, and the M.Sc. and Ph.D. degrees in electrical engineering from the University of Arkansas, Fayetteville, AR, USA, in 2008 and 2011, respectively. In 2012, he joined the Photonics Group as a Research Associate on Molecular Beam Epitaxy of III–V compound semiconductors and optoelectronic devices. Since October 2015, he has been a Lecturer in the Department of Electronic and Electrical Engineering, University College London, London, U.K.

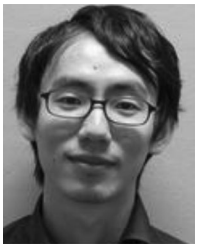

Qi Jiang received the B.Sc. degree in electronics from the University of Sheffield, Sheffield, U.K., in 2004, and the M.Sc. degree in a joint venture between University of Sheffield and University of Leeds, Leeds, U.K., in 2005. He started the Ph.D. degree in the topic of quantum dot laser and superluminescent diode in 2008 at the Department of Electronic and Electrical Engineering after he worked with the Department of Physics in the University of Sheffield. He is currently a Research Associate at the University College London, London, U.K., where he is working in the integration of Group IV and III–V photonics.

Ken Kennedy received the B.Sc. degree in optoelectronics from Heriot–Watt University, Edinburgh, U.K., in 1999 and the Ph.D. degree in electronic and electrical engineering from the University of Sheffield, Sheffield, U.K., in 2009. He immediately joined Hewlett Packard, Ipswich, U.K., as a Manufacturing/R&D Engineer working on telecom wavelength emitters and detectors. In 2004, he joined Agilent Technologies Ltd., Singapore as a Technology Transfer Engineer. After graduating, he received a Post Doctoral Prize Fellowship, funded by the EPSRC, working mainly on quantum cascade laser technologies. He currently works for the EPSRC National Centre for III–V Technologies, University of Sheffield and is responsible for the device fabrication of a variety of devices and materials. His research interests include semiconductor laser and emitter technologies.

Pamela Jurczak received the M.Eng. degree in electronic and electrical engineering with nanotechnology from University College London (UCL), London, U.K., in 2014. She is currently working toward the Ph.D. degree at Molecular Beam Epitaxy Research Group, UCL. Her research interest includes III–V and Group-IV MBE materials growth for thermophotovoltaic cells and nanowires.

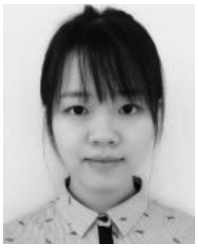

Mengya Liao received the B.Eng. degree (First-Class Hons.) in electronic and electrical engineering from University College London (UCL), London, U.K., in 2015. Since September 2015, she has been working toward the Ph.D. degree with the Photonics Group, UCL. Her current research interests include optoelectronic device fabrication and molecular beam epitaxy of III–V compound semiconductors.

Richard Beanland received the Ph.D. degree from the University of Liverpool, Liverpool, U.K. He spent over a decade working on structural characterization of III–V devices at GEC-Marconi (later Bookham Technology). He is currently the Director of electron microscopy at Warwick University, Coventry, U.K., and works on a wide range of topics including III–V materials, functional oxides, electron diffraction, and aberration-corrected TEM.

Alwyn Seeds received the B.Sc., Ph.D., and D.Sc. degrees from the University of London, London, U.K. From 1980 to 1983, he was a Staff Member at Lincoln Laboratory, Massachusetts Institute of Technology, Cambridge, MA, USA, where he worked on GaAs monolithic millimetre-wave integrated circuits for use in phased-array radar. Following three years as a Lecturer in telecommunications at Queen Mary College, University of London, he moved to University College London in 1986, where he is currently a Professor of optoelectronics and the Head of the Department of Electronic and Electrical Engineering. He has published more than 350 papers on microwave and optoelectronic devices and their systems applications. His current research interests include semiconductor optoelectronic devices, wireless and optical communication systems.

He is a Fellow of the Royal Academy of Engineering (U.K.). He has been a Member of the Board of Governors and the Vice-President for Technical Affairs of the IEEE Photonics Society (USA). He has served on the program committees for many international conferences. He is a cofounder of Zinwave, a manufacturer of wireless over fibre systems. He received the Gabor Medal and Prize of the Institute of Physics in 2012.

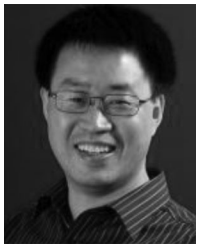

Huiyun Liu received the Ph.D. degree in semiconductor science from the Institute of Semiconductor, Chinese Academy of Sciences, Beijing, China. After receiving the Ph.D. degree, he joined the EPSRC National Centre for III–V Technologies at University of Sheffield, Sheffield, U.K., in August 2001. He was responsible for the development of molecular beam epitaxy growth of semiconductor materials for the U.K. academic and industrial research community. In 2007, he was awarded Royal Society University Research Fellow and started his academic career in the Department of Electronic and Electrical Engineering at University College London (UCL), London, U.K., where he is currently a Professor of semiconductor photonics. He has coauthored more than 300 papers in the area of semiconductor materials and devices. His general interest include the nanometre-scale engineering of low-dimensional semiconductor structures (such as quantum dots, quantum wires, and quantum wells) by using molecular beam epitaxy and the development of novel optoelectronic devices including lasers, detectors, and modulators by developing novel device process techniques.